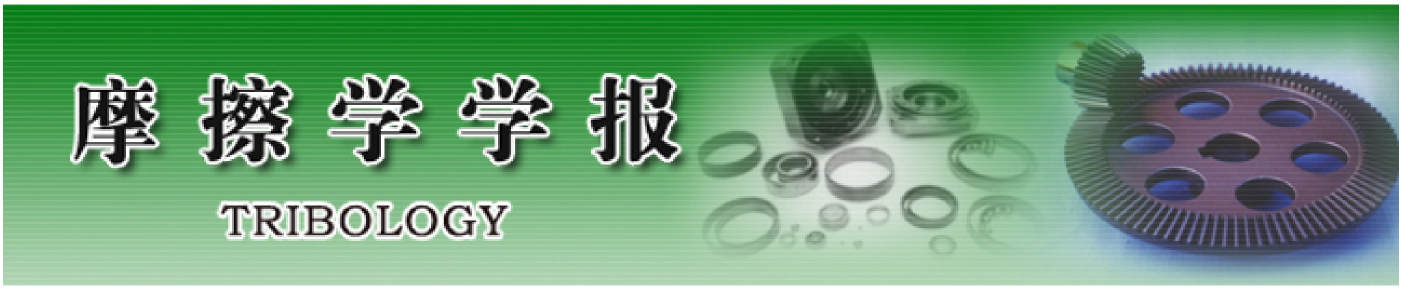

高黏度液体热膨胀系数和压缩弹性模量的测量方法研究

孙朝阳，方静泊，陈文庆，曹辉，白鹏鹏，田煜

Measurement Method of Coefficient of Thermal Expansion and Compressive Elastic Modulus of Highly Viscous Liquids

SUN Zhaoyang, FANG Jingbo, CHEN Wenqing, CAO Hui, BAI Pengpeng, TIAN Yu

在线阅读 View online: https://doi.org/10.16078/j.tribology.2024208

第 46 卷　第 1 期
2026 年 1 月

摩擦学学报（中英文）
Tribology

Vol 46　No 1
Jan, 2026

孙朝阳, 方静泊, 陈文庆, 曹辉, 白鹏鹏, 田煜. 高黏度液体热膨胀系数和压缩弹性模量的测量方法研究[J]. 摩擦学学报（中英文）, 2026, 46(1): 1−9.　SUN Zhaoyang, FANG Jingbo, CHEN Wenqing, CAO Hui, BAI Pengpeng, TIAN Yu. Measurement Method of Coefficient of Thermal Expansion and Compressive Elastic Modulus of Highly Viscous Liquids[J]. Tribology, 2026, 46(1): 1−9.　DOI: 10.16078/j.tribology.2024208

高黏度液体热膨胀系数和压缩弹性模量的测量方法研究

孙朝阳, 方静泊, 陈文庆, 曹　辉, 白鹏鹏, 田　煜*
(清华大学 高端装备界面科学与技术全国重点实验室，北京 100084)

摘　要: 热膨胀系数和压缩弹性模量是液体密度温变和压变特性的重要物理参数，热膨胀系数和压缩弹性模量变化会影响对实际工况下密封和润滑失效等问题理论分析准确度. 针对高黏度润滑油的阻尼效应严重影响现有商用振动弦式密度计的激振，难以实现高精度测定的问题，本文中设计了1种采用因瓦合金作为罐体材料及小内径毛细管计量膨胀体积的测量装置，直接测定温升过程中液体的膨胀体积和密封罐体中液体的膨胀压强，隔绝高黏度液体的阻尼效应对测定的影响. 装置的密度测定精准度为±0.05%，热膨胀系数和压缩弹性模量测定精准度可以达到±3%. 测定部分PAO基础油，从室温到80 ℃，其热膨胀系数升高近30%，30~45 ℃压缩弹性模量约为1.28~1.45 GPa. 本研究中设计的测定装置可以实现高黏度润滑油热膨胀系数和压缩弹性模量高精准测定，可为润滑油理论分析计算所需参数提供更可靠的基础数据支撑.

关键词: 热膨胀系数; 压缩弹性模量; 密度; 高黏度润滑油; PAO基础油
中图分类号: TH117.1　　**文献标志码:** A　　**文章编号:** 1004-0595(2026)01–0001–09

Measurement Method of Coefficient of Thermal Expansion and Compressive Elastic Modulus of Highly Viscous Liquids

SUN Zhaoyang, FANG Jingbo, CHEN Wenqing, CAO Hui, BAI Pengpeng, TIAN Yu*

(*State Key Laboratory of Tribology in Advanced Equipment, Tsinghua University, Beijing 100084, China*)

Abstract: The coefficient of thermal expansion and the modulus of elasticity in compression are important physical parameters for the temperature and compressive behavior of the density of liquid lubricants. Changes in the coefficient of thermal expansion and the modulus of elasticity in the compression of lubricants affect the accuracy of theoretical analyses of problems such as sealing and lubrication failures under actual operating conditions. Existing commercial vibrating string densitometers can measure the temperature and pressure characteristics of low-viscosity liquid density with high accuracy, but the damping effect of high-viscosity lubricants seriously affects the vibrating string excitation, and the measurement error is large. In this paper, a device was designed to measure the coefficient of thermal expansion and compressive elastic modulus of high-viscosity lubricating oils using Invar alloy as the tank material and a small internal diameter capillary metering expansion volume, with an accuracy of ±0.05% for density measurement and ±3% for coefficient of thermal expansion and compressive elastic modulus measurement. PAO8, PAO10 and PAO65 were selected as the base oils for the determination of the coefficient of thermal expansion from room temperature to 80 ℃

Received 24 September 2024, revised 26 December 2024, accepted 30 December 2024, available online 28 January 2026.
*Corresponding author. E-mail: tianyu@mail.tsinghua.edu.cn. Tel: +86-10-62789482.
This work was supported by the National Natural Science Foundation of China (52275198, 52205206)
国家自然科学基金项目(52275198, 52205206)资助.

and the compressive elastic modulus at room temperature. The coefficient of thermal expansion of base oil from room temperature to 80 ℃ was about 7×10^{-4}~10×10^{-4}/℃, which increased by nearly 30%. The compressive elastic modulus of the base oil was about 1.28~1.45 GPa, which decreased slightly with the increase in temperature. The device designed in this study for the determination of the coefficient of thermal expansion and compressive elastic modulus of lubricating oil filled the gap in the accurate determination of the coefficient of thermal expansion and compressive elastic modulus of high viscosity lubricating oil, and it could provide support for the theoretical analysis of lubricating oils to calculate the required parameters.

Key words: coefficient of thermal expansion; modulus of elasticity in compression; density; high viscosity lubricants; PAO base oils

在航空航天发动机和液压系统等高端装备领域存在大量的高副接触[1]，润滑油往往工作在高温和重载等极端工况条件下[2-5]. 高温高压下，润滑油的热膨胀系数和压缩弹性模量是决定润滑油性能的关键参数[6-7]，热膨胀系数和压缩弹性模量是描述随温度和压强变化，液体润滑剂体积和密度变化趋势的基本物理量[8-11]. 过高的热膨胀系数会影响实际油膜厚度的理论分析计算，也会增加泄露风险[12]. 高压缩弹性模量的润滑油在高温高压下能更好地抵抗压缩，在高压下形成有效稳定的油膜，并维持足够的油膜厚度，保持其黏度和流动特性. 过低的压缩弹性模量会导致润滑油在高压下过度变形，影响润滑油膜的形成和稳定性[13-15].

热膨胀系数的科学研究始于固体因瓦合金的研制，1933年瑞典国际计量局纪尧姆在“INVAR”的报道文章中指出可以制造热膨胀系数小于1.6×10^{-6}/℃的因瓦合金(Invar) [16-17]，研究者对水密度的认识也始于热膨胀系数的测定. 由于固体具有明显的边界，所以固体热膨胀系数和压缩弹性模量的测定已经具有成熟的体系[18-21]，气体可以通过范德华气体状态方程分析气体温变和压变特性[22]，对液体热膨胀系数和压缩弹性模量的测定通常需要固体容器承载，这会显著影响液体热膨胀系数测定精准度. 现有对液体直接测定研究中，Strachala等[23]通过阿基米德浮力法和阿贝折射仪测定液体的密度计算热膨胀系数，测定的相对误差为10%. Mikhailov等[24]通过对试验测定液体的密度拟合，对液体的热膨胀系数进行拟合计算，测定的相对误差在±5%范围. Lane等[25]通过激光测定液体的压缩弹性模量，对水等液体的测定精准度约为10%. 直接测量方法对液体介质要求不高，可以测定高黏度液体、悬浊液和混合液体，但精准度较低. 振动弦法可以实现液体密度温变和压变特性的高精准和快速测定[26-27]，但只能保证低黏度液体的测定精准度[28]. 由此导致高黏度润滑油热膨胀系数和压缩弹性模量的装置和试验数据匮乏，难以实现热膨胀和压缩弹性模量的精准测定[29-32]，不能为实际理论分析提供精确的数据支撑.

本文中设计了1种采用因瓦合金作为罐体材料及小内径毛细管计量膨胀体积来精密测量润滑油热膨胀系数的装置，采用升温加压的方式简化液体压缩弹性模量测定装置. 对基础油PAO8、PAO10和PAO65进行热膨胀系数和压缩弹性模量测定，得到同种润滑油热膨胀系数和压缩弹性模量同温度和黏度的相关关系. 本研究中设计的高黏度润滑油热膨胀系数和压缩弹性模量的测定装置可为高黏度润滑油理论分析计算提供数据支撑.

1 试验部分

1.1 试验仪器

液体体积随温度的变化是分子间距变化的宏观体现，当温度升高，分子的动能增加，加剧分子的无规则运动，导致分子间的平均距离增加. 当液体不受限，测定一定温升下液体的膨胀体积可以计算热膨胀系数. 当液体受限，此时升高温度，分子间碰撞更加剧烈，导致内部压强上升，由此通过测定受限液体的压强变化，可以计算出液体压缩弹性模量.

基于上述原理搭建了液体热膨胀系数和压缩弹性模量的测量装置，图1(a)和(b)所示为热膨胀系数和压缩弹性模量装置结构图. 热膨胀系数测定为非密闭罐体，通过毛细管实时显示液体膨胀体积. 压缩弹性模量测定为密封罐体，测定被测液体升温对罐体产生的压强作用. 选用压强传感器P和温度传感器T测定压强和温度返回值.

为提高装置测定精确度及实现参数的自动化测定，分别从装置材料、尺寸和测定方法进行优化设计. $V_{\rm tank}$和$V_{\rm liquid}$分别为实际罐体体积和罐体所能装载液体体积，以PAO8基础油作为测定液体，对比采用因瓦合金材料和铝合金作为罐体材料，采用因瓦合金作为罐体材料相对误差将从5.22%降低到0.36%，极大提高装置测定精准度，如图2(a)所示. 如图2(b)所示，基于

传感器的数值反馈，该装置可以实现热膨胀系数和压缩弹性模量的连续自动化测量. 如图2(c)所示，设计大内径承载罐体d_2和小内径毛细管d_1. 当液体膨胀一定体积，成在罐体和毛细管上升高度分别对应为Δh_2和Δh_1. 增大内径比，液体受热膨胀引起液面高度的上升可以通过毛细管以100倍的反馈比进行显示. 图2(d)所示为采用升温加压的方式测定被测液体的压缩弹性模量，对比传统直接加压方式，降低了装置的繁琐程度，对比直接加压方式需要手动计算压缩体积，升温加压方式采用测定的热膨胀系数直接计算压缩弹性模量.

1.2　测量方法

液体热膨胀系数的测定采用液体升温自由膨胀，如图1(a)所示，液体初始体积V_1，初始温度T_1，升高一定温度，液体体积和温度变为V_2和T_2. 即在该温度段内的热膨胀系数为:

$$\alpha = \frac{V_2 - V_1}{(T_2 - T_1)V_1} = \frac{\Delta V}{\Delta T V_1} \tag{1}$$

热膨胀系数测定中采用温度传感器检测温度变化，压强传感器通过检测液面高度差引起的压强差，计算液面上升高度，从而得到液体膨胀体积. 毛细管内径为d_1，升高一定温度，液面上升高度Δh，此时膨胀液体体积ΔV为

$$\Delta V = \frac{\pi {d_1}^2}{4}\Delta h \tag{2}$$

液面上升高度Δh通过压强传感器检测压强差Δp计算，$\Delta p = \rho g \Delta h$，其中$g$和$\rho$分别为重力加速度和液体密度. 液体密度随温度和压强变化，在实际测定过程中采用前一个数据点密度计算下一个数据点密度，其中温度数据点间隔为0.1 ℃，由此实时计算在当前温度和压强下的密度值.

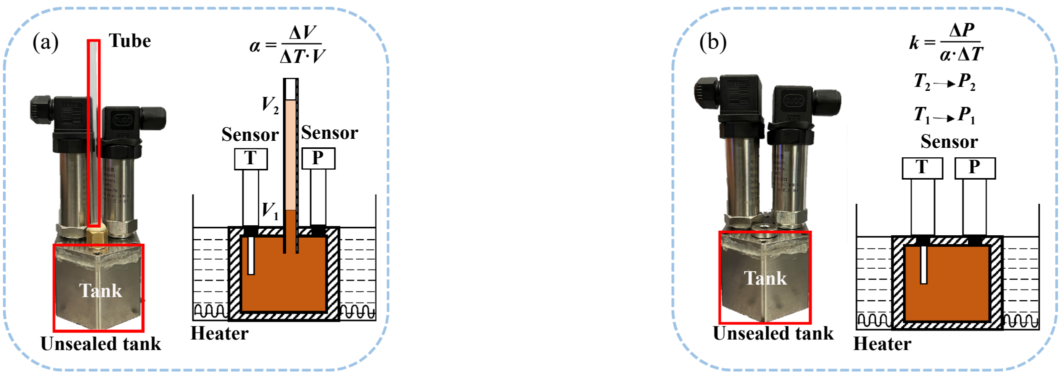

Fig. 1　Device structure: (a) thermal expansion instrument structure; (b) compressive modulus of elasticity device structure

图 1　装置结构: (a)热膨胀系数装置结构; (b)压缩弹性模量装置结构

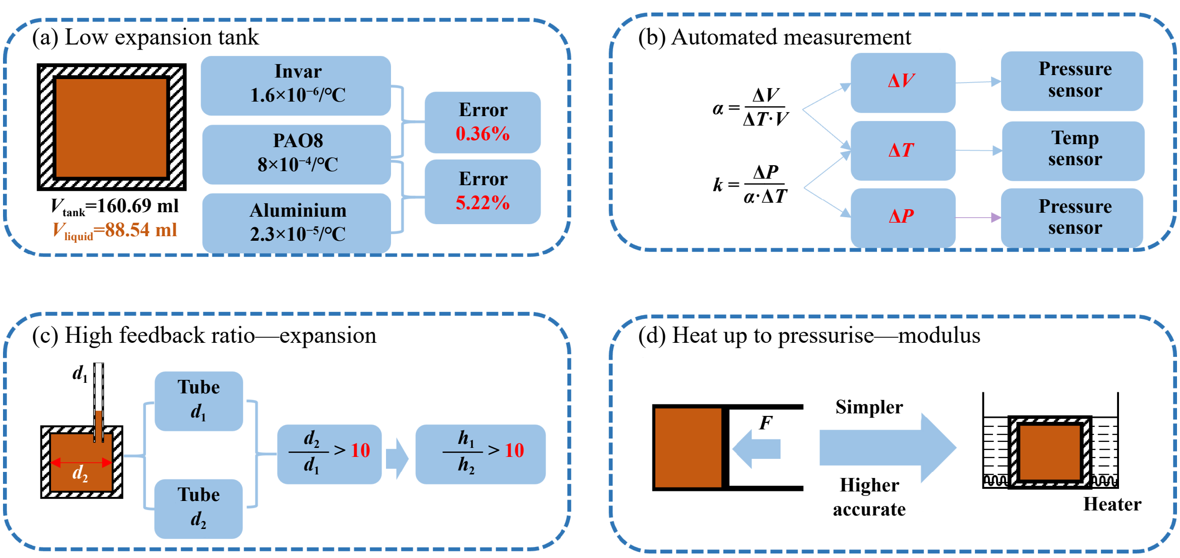

Fig. 2　Device design: (a) invar tank design; (b) automated measurement of device design; (c) high diameter ratio capillary glass tube design; (d) heat up to pressurize design

图 2　装置设计: (a)因瓦合金罐体设计; (b)装置自动化测定设计; (c)高直径比毛细玻璃管设计; (d)升温加压设计

根据液面压强差计算液体密度，根据测定过程中的重量守恒，设定被测液体的质量为m，初始体积V_1，初始密度ρ. 加热后密度ρ_Δ，及膨胀体积ΔV，过程中密度为

$$\begin{cases}\rho = \dfrac{m}{V_1}\\ \rho_\Delta = \dfrac{m}{V_1+\Delta V}\end{cases} \tag{3}$$

结合分析式(2)和式(3)，可以通过压强传感器返回压强值Δp和相关已知参数，计算当前温度下的液体密度

$$\rho_\Delta = \rho - \frac{\pi d_1^{\,2}\Delta p}{4gV_1} \tag{4}$$

基于式(4)可以通过温度传感器和压强传感器返回数值，计算液体密度随温度变化的曲线. 在曲线上任选两个密度值ρ_n和ρ_m，对应体积V_n和V_m，对应温度值T_n和T_m，其中T_m大于T_n. 热膨胀系数α关系如下

$$\begin{cases}\Delta V = V_m - V_n\\ \Delta V = \alpha V_n(T_m - T_n)\end{cases} \tag{5}$$

基于式(5)计算热膨胀系数为

$$\alpha = \frac{\rho_n-\rho_m}{\rho_m(T_m-T_n)} = -\frac{1}{\rho}\frac{d\rho}{dT} \tag{6}$$

根据压强传感器返回值ΔP、温度变化ΔT以及该温度下的热膨胀系数α，得到液体在该测定温度和该测定压强的压缩弹性模量k为

$$k = \frac{\Delta P}{\alpha\Delta T} \tag{7}$$

装置的测量流程示意图如图3所示，图3左侧步骤a1~步骤a3为热膨胀系数测定的流程图，图3右侧步骤b1和步骤b2为压缩弹性模量测定流程图. 其中步骤a1和b1为被测液体的装填和罐体装配密封. 在测定热膨胀系数步骤中a2为液体室温密度标定，标定液体室温常压下的密度值. 在步骤a2中，在毛细管中滴加一定体积的被测液体，测定返回压强和滴加液体高度，通过$\Delta p=\rho g\Delta h$计算室温液体密度. 步骤a3中，通过水浴加热，使罐体均匀受热，采集升温过程中的返回温度值和压强值，根据式(4)和式(6)计算液体不同温度下的密度和热膨胀系数. 压缩弹性模量测定中，步骤b2采集密封罐体升温过程中的压强返回值和温度返回值，以及结合热膨胀系数测定过程中得到的热膨胀

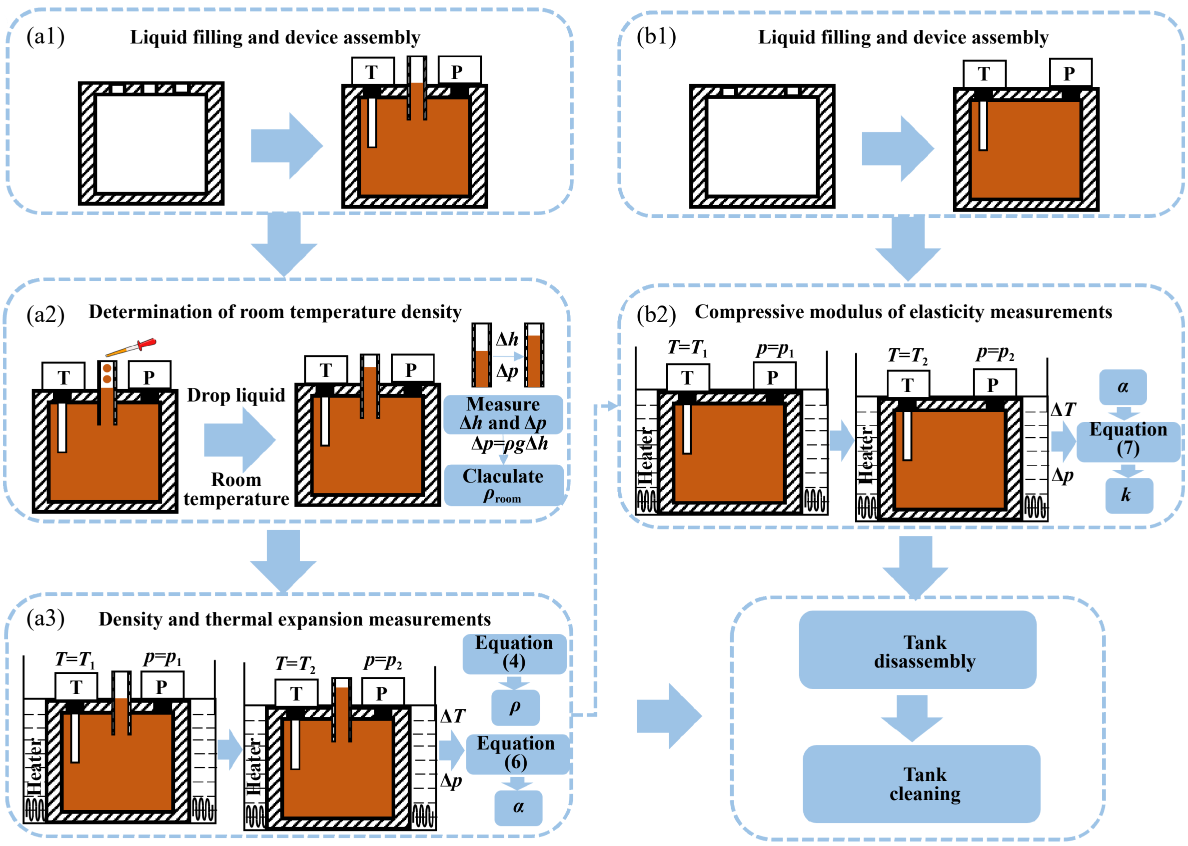

Fig. 3 Schematic diagram of the measurement process of the device

图 3 装置测量流程示意图

系数，根据式(7)计算压缩弹性模量，测定过后需要进行装置的清洗.

1.3　试验试剂

试验中，去离子水和季戊四醇四乙基己酸脂作为仪器精准度检测液体. 季戊四醇四乙基己酸脂(PEB8)购自麦克林试剂，基础油PAO8和PAO10购自美国雪佛龙润滑油公司，基础油PAO65购自美孚公司. 所有测定液体试验前均抽取真空，减少液体内部气泡对试验结果的影响.

2　结果与讨论

2.1　装置一致性及精准度分析

以去离子水作为核验该装置一致性和精准度检测液体，图4所示为热膨胀系数装置一致性及精准度测试图. 图4(a)所示为测定水的温度-密度曲线，液体温度-密度的斜率一定程度代表热膨胀系数的大小，即密度梯度表征液体的热膨胀系数. 图4(b)所示为测定水的温度-热膨胀系数曲线，用装置进行3次试验测定水的密度和热膨胀系数，对比均值和误差带，最大相对误差为±0.01%. 图4(a)和(b)中标示参考文献中去离子水的密度和热膨胀系数[33-34]，参考标准水的密度和热膨胀系数均在测定结果误差棒范围内，说明该仪器测定结果精准度较高. 图4(c)所示为水密度测定的相对误差，蓝色框线内代表误差为±0.05%. 图4(d)所示为水热膨胀系数测定的相对误差，蓝色框线内代表误差为±2.5%.

多次测定水在25~35 ℃下的压缩弹性模量，该装置测定水的压缩弹性模量结果列于表1中. 对比标准水的压缩弹性模量[35-36]，计算相对误差为2.71%.

振动弦式密度计通过黏度系数校正，可以实现低黏度润滑油高精准度测定[28, 37]，但随着黏度升高，校正效果欠佳. PEB8润滑油在40 ℃下的黏度为41.73 mPa·s[38]，采用该装置测定PEB8润滑油和校正后的振动弦式密度计测定结果对比列于表2和表3中.

综合对比水和PEB8测定对比结果，对密度的测定结果较均匀分散在±0.05%的误差带中，对热膨胀结果的测定精度可以保持在±2.0%，存在部分结果略高于此误差，但总体均能保持在±2.5%以内. 对压缩弹性模量的测定结果，一般维持在±3.0%以内. 该装置通过直接测定润滑油膨胀体积和升温压强，属于物质基本

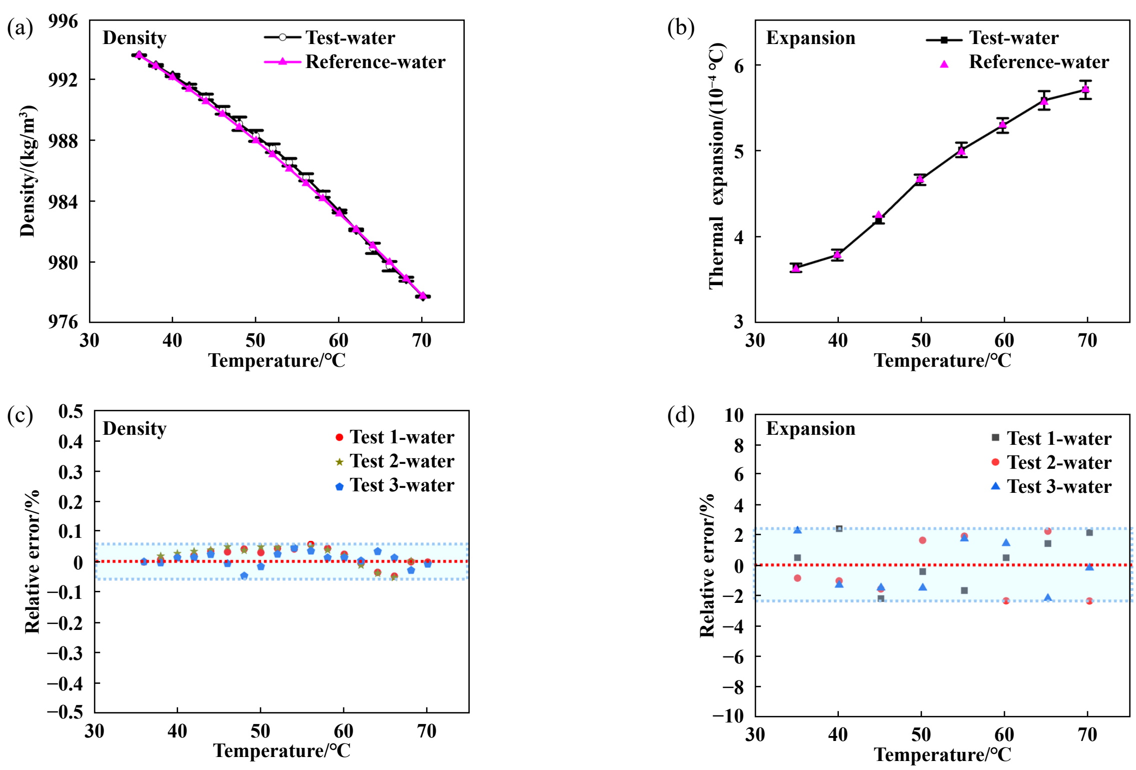

Fig. 4　Coefficient of thermal expansion device consistency and accuracy test chart: (a) determination of the density of water; (b) determination of the coefficient of thermal expansion of water; (c) relative error of water density determination; (d) relative error of thermal expansion of water

图 4　热膨胀系数装置一致性及精准度测试图: (a)水的密度测定; (b)水的热膨胀系数测定; (c)水密度测定相对误差; (d)水热膨胀系数测定相对误差

表 1 水的压缩弹性模量测定

Table 1 Determination of the compressive elastic modulus of water

Experiment	Compression modulus
Test	2.15 GPa
Reference[35-36]	2.21 GPa
Relative Error	2.71%

物性，测定结果不受液体黏度等因素限制. 通过去离子水和PEB8测定结果的准确度对比，说明装置测定精准度是可信的. 热膨胀系数测定和压缩弹性模量的测定均需要对罐体升温，固体的热膨胀没有方向性，罐体自身的膨胀会对测定造成直接影响. 压强传感器的测定精度直接影响热膨胀系数测定中的液面高度测定和压缩弹性模量中的压强测定. 由此，罐体自身的膨胀和压强传感器的精度是影响该装置精度的主要因素.

在热膨胀系数测定中，测定液体的热膨胀系数越小，罐体的热膨胀$\alpha_{\rm tank}$对液体热膨胀系数$\alpha_{\rm liquid}$测定影响越大，基于该装置罐体体积$V_{\rm tank}$和承载液体体积$V_{\rm liquid}$，某一测定温度下，罐体热膨胀的影响为$\dfrac{\alpha_{\rm tank}V_{\rm tank}}{\alpha_{\rm liquid}V_{\rm liquid}}$. 以室温下的水和PAO8为例，罐体自身热膨胀对热膨胀系数的测定分别带来约±0.96%和±0.36%的误差. 传感器测定液面高度，假定传感器量程和精度为P和γ，则测定液面高度的精度为$\dfrac{P\gamma}{\rho g}$，其中ρ和g分别为液体密度和重力加速度. 由此对液体热膨胀系数测定的影响为$\dfrac{P\gamma S}{\rho g\alpha_{\rm liquid}V_{\rm liquid}}$，其中$S$为毛细管截面积. 以该装置2 kPa量程，精度0.2%压强传感器和室温下的PAO8为例，压强传感器对液面高度识别精度为0.4 mm，对热膨胀系数测定带来±0.39%误差. 压缩弹性模量测定中，主要是压强传感器精度对实际测量存在影响.

2.2 基础油热膨胀系数及压缩弹性模量测定

采用该装置对高黏度PAO基础油进行热膨胀系数和压缩弹性模量测定，图5所示为PAO基础油热膨胀系数测定图. 图5(a)、(b)和(c)分别为基础油膨胀体积和热膨胀系数测定图，温度对热膨胀系数影响较大. 基础油由室温25 ℃升高到80 ℃，热膨胀系数上升30%左右. PAO8和PAO10的热膨胀系数较接近，要远大于PAO65的热膨胀系数. 由此PAO基础油随着黏度的升高，其热膨胀系数有一定程度降低，该现象在同一种润滑油中热膨胀温升曲线中也得到解释. 以PAO8为例，PAO8的热膨胀系数随温度升高而升高，但PAO8的黏度随温度上升而降低，即对于同一种类的基础油，润滑油黏度和热膨胀系数之间存在一定的负关联性[41-42].

该装置可以较好地实现高黏度润滑油的热膨胀系数测定，其中常温和低剪切速率下PAO65的黏度高于1 Pa·s. 对比振动弦式密度计仅能精准测定低黏度液体，该热膨胀测定装置可以高效精准测定高黏度润滑油热膨胀系数和压缩弹性模量. 30 ℃下测定PAO8、PAO10和PAO65润滑油的压缩弹性模量并列于表4中，压缩弹性模量随着基础油黏度的增加而下降. 图6所示为基础润滑油压缩弹性模量测定图，图6(a)所示为以5 ℃为间隔计算基础油的压缩弹性模量，该压缩弹性模量一定程度和黏度相关，即随黏度升高，压缩弹性模量变大. 对比图6(b)中30 ℃下的压缩弹性模量，PAO10比PAO8高6%，PAO65比PAO10高7%. 液体的压缩模量是随温度和压强变化的参量，在此装置中仅测定在20 MPa以下压强的液体压缩弹性模量，由此在此仅考虑在该范围内液体压缩弹性模量随温度变化. 对比经过黏度校正的振动弦式PAO8测定数据，该装置对PAO8测定数据精准度在所述精度内[43].

3 结论

本文中通过选用因瓦合金罐体、毛细管显示膨胀体积和升温加压方式设计高黏度润滑油热膨胀系数

表 2 PEB8热膨胀系数测定对比

Table 2 Comparison of PEB8 coefficient of thermal expansion measurement

Parameters	25 ℃	35 ℃	45 ℃
Coefficient of thermal expansion in test/(10^{-4}/℃)	7.26	7.42	7.85
Coefficient of thermal expansion in reference[39-40]/(10^{-4}/℃)	7.18	7.27	7.83
Relative Error	1.11%	2.06%	0.26%

表 3 PEB8压缩弹性模量测定对比

Table 3 Comparison of PEB8 compressive modulus of elasticity determination

Parameters	25 ℃	35 ℃	45 ℃
Compressive modulus of elasticity in test/GPa	1.57	1.52 (1.524)	1.43
Compressive modulus of elasticity in reference[39-40]/GPa	1.61	1.52 (1.520)	1.45
Relative Error	2.48%	0.26%	1.38%

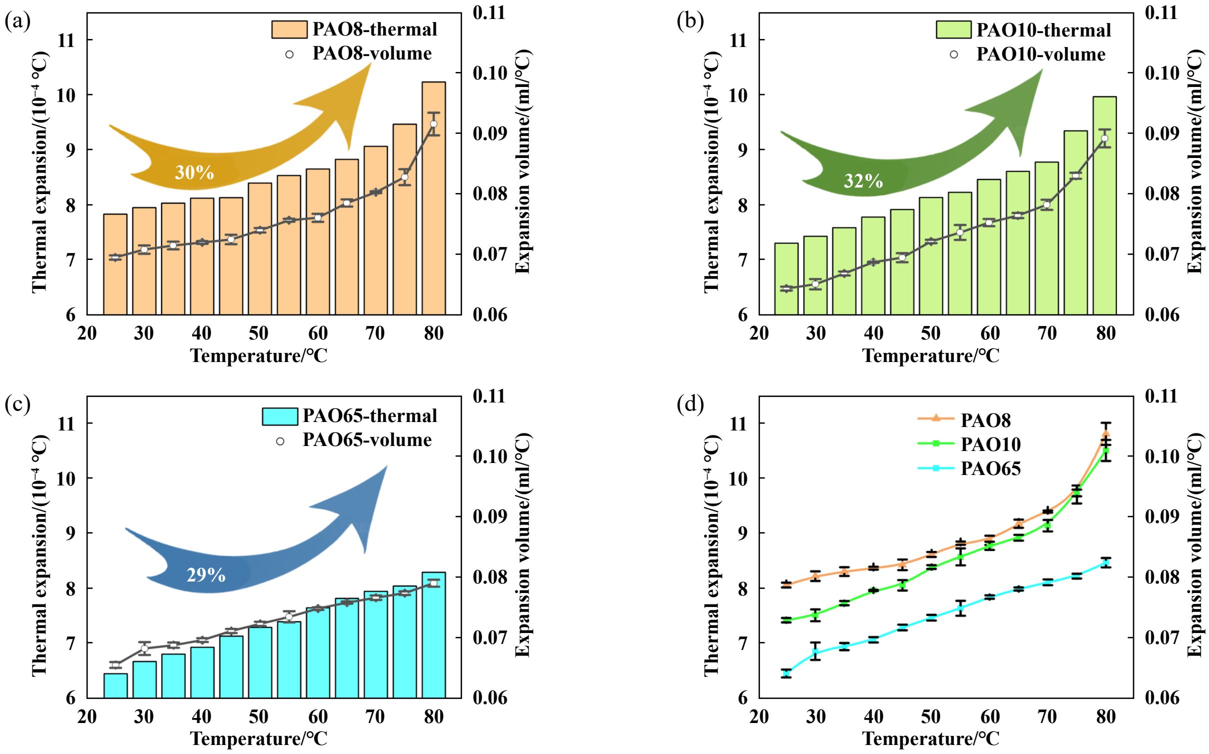

Fig. 5　Determination of coefficient of thermal expansion of PAO base oil: (a) PAO8; (b) PAO10; (c) PAO65; (d) coefficient of thermal expansion of PAO base oil

图 5　PAO基础油热膨胀系数测定: (a) PAO8; (b) PAO10; (c) PAO65; (d) PAO基础油热膨胀系数

表 4　基础油温升压强及压缩弹性模量

Table 4　Base oil temperature rise pressure and compression modulus of elasticity

Oil	PAO8	PAO10	PAO65
Compressive modulus of elasticity/GPa	1.287	1.360	1.452

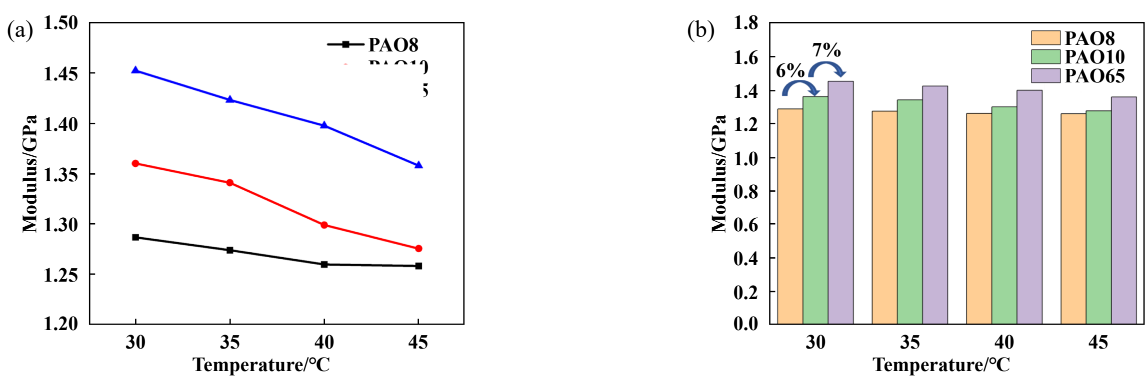

Fig. 6　Determination of base oil compression elastic modulus: (a) base oil compression modulus of elasticity; (b) base oil compression modulus comparison

图 6　基础油压缩弹性模量测定: (a)基础油压缩弹性模量; (b)基础油压缩弹性模量对比

和压缩弹性模量的测定装置, 可以实现高黏度润滑油在25~80 ℃温度下的热膨胀系数以及在温度为30~45 ℃、压强为0~20 MPa条件下的压缩弹性模量测定, 精确度在3%以内. 基于该仪器对部分基础油PAO进行测定. 对测定装置和测定结果得出结论如下:

a. 通过水和PEB8油的精准度检测, 得到装置的测定密度精准度在±0.05%范围, 热膨胀系数测定精准度在±2.5%范围, 压缩弹性模量测定装置精准度可以保持在±3%以内, 对比直接测量装置精准度提高40%, 对比振动弦式方法可以测定1 Pa·s的高黏度润滑油.

b. 对PAO8、PAO10和PAO65等油品进行测定，得到室温到80 ℃，其热膨胀系数约为7×10^{-4}~10×10^{-4}/℃，升高近30%；30~45 ℃温度范围内其压缩弹性模量约为1.28~1.45 GPa. 在测定中发现基础油热膨胀系数与温度存在正关联性，与黏度存在负关联性，基础油压缩弹性模量同黏度存在正关联性.

参 考 文 献

[1] Guan Bowen, Gong Shi, Zhang Feng, et al. Friction and wear mechanism of silver-coated layer of aviation hydraulic plunger pump's slipper[J]. Tribology, 2024, 44(10): 1323–1333 (in Chinese) [管博文, 龚适, 张峰, 等. 航空液压柱塞泵滑靴镀银层摩擦磨损机理研究[J]. 摩擦学学报(中英文), 2024, 44(10): 1323–1333]. doi: 10.16078/j.tribology.2023158.

[2] Hu Ningning, Zhang Xiuheng, Chen Peng, et al. High temperature tribological properties and curve fitting of silver pyrazole methylpyridine complex as lubricating oil additive[J]. Tribology, 2023, 43(12): 1434–1444 (in Chinese) [胡宁宁, 张修恒, 陈鹏, 等. 银吡唑甲基吡啶配合物复合润滑油添加剂的高温摩擦学性能研究与曲线拟合[J]. 摩擦学学报, 2023, 43(12): 1434–1444]. doi: 10.16078/j.tribology.2022201.

[3] Wu Bi, Zhang Zhenbo, Li Shu. Advances in tribology of aero-engine materials[J]. Tribology, 2023, 43(10): 1099–1117 (in Chinese) [吴彼, 张振波, 李曙. 航空发动机材料摩擦学研究进展[J]. 摩擦学学报, 2023, 43(10): 1099–1117]. doi: 10.16078/j.tribology.2023226.

[4] Wu Kun, Jiang Xufeng, Fei Yiwei, et al. Comparative analysis of anti-foaming performance of two kinds of aviation lubricating oils under high-temperature oxidation condition[J]. Lubrication Engineering, 2019, 44(12): 101–107 (in Chinese) [吴坤, 姜旭峰, 费逸伟, 等. 两种航空润滑油高温氧化条件下抗泡性能对比分析[J]. 润滑与密封, 2019, 44(12): 101–107]. doi: 10.3969/j.issn.0254-0150.2019.12.018.

[5] Zhao Hui, Shan Lei, Cao Hui, et al. Tribological behavior of 15# aviation hydraulic oil[J]. Tribology, 2024, 44(08): 1136–1150 (in Chinese) [赵辉, 山磊, 曹辉, 等. 15#航空液压油的摩擦磨损性能研究[J]. 摩擦学学报(中英文), 2024, 44(08): 1136–1150]. doi: 10.16078/j.tribology.2023210.

[6] Zhang Enhui, Li Weimin, Zhao Gaiqing, et al. The influence of viscosity of mineral oil in the microstructure and performances of lithium-based greases[J]. Tribology, 2022, 42(6): 1258–1266 (in Chinese) [张恩惠, 李维民, 赵改青, 等. 不同黏度矿物基础油对锂基润滑脂微观结构及性能的影响研究[J]. 摩擦学学报, 2022, 42(6): 1258–1266]. doi: 10.16078/j.tribology.2021242.

[7] Lu Hang, Hua Jing, Hu Meng, et al. Development of the properties and application of glycerol-based green lubricant[J]. Tribology, 2024, 44(11): 1614–1638 (in Chinese) [陆航, 花镜, 胡盟, 等. 甘油基绿色润滑剂的性能与应用研究进展[J]. 摩擦学学报(中英文), 2024, 44(11): 1614–1638]. doi: 10.16078/j.tribology.2023217.

[8] Tipler P A, Mosca G. Physics for scientists and engineers[M]. New York: Worth Publishers, 2008.

[9] Song Changsheng, Xu Lei, Tang Yadan, et al. Effect of viscosity on the density detection of lubricating oils[J]. Lubricating Oil, 2016, 31(3): 39–41 (in Chinese) [宋昌盛, 徐磊, 唐亚丹, 等. 黏度对润滑油密度测定准确性的影响[J]. 润滑油, 2016, 31(3): 39–41]. doi: 10.19532/j.cnki.cn21-1265/tq.2016.03.010.

[10] Liu Zikui, Wang Yi, Shang Shunli. Thermal expansion anomaly regulated by entropy[J]. Scientific Reports, 2014, 4: 7043. doi: 10.1038/srep07043.

[11] Liu Zikui, Wang Yi, Shang Shunli. Origin of negative thermal expansion phenomenon in solids[J]. Scripta Materialia, 2011, 65(8): 664–667. doi: 10.1016/j.scriptamat.2011.07.001.

[12] Hashim W M, Al-Salihi H A, Al Zubaidi F N. Effects of temperature on the properties of HL32 oil in the conventional hydraulic actuators[J]. Heliyon, 2022, 8(12): e11831. doi: 10.1016/j.heliyon.2022.e11831.

[13] Zheng Que, Cheng Xiang, Zuo Zheqing, et al. The influence analysis of the elastic modulus on the damping characteristics of hydraulic dampers[J]. Chinese Hydraulics & Pneumatics, 2019(9): 123–126 (in Chinese) [郑悫, 程相, 左哲清, 等. 液体弹性模量对减摆器阻尼特性影响的研究[J]. 液压与气动, 2019(9): 123–126]. doi: 10.11832/j.issn.1000-4858.2019.09.020.

[14] Hu Kai, Zhang Wenyi. Analysis and optimization of dynamic characteristics of closed hydraulic system under different bulk elastic modulus of oil[J]. Machine Tool & Hydraulics, 2020, 48(16): 136–139 (in Chinese) [扈凯, 张文毅. 不同油液体积弹性模量下闭式液压系统动态特性分析及优化[J]. 机床与液压, 2020, 48(16): 136–139]. doi: 10.3969/j.issn.1001-3881.2020.16.028.

[15] Li Jiabao, Gu Lichen, Sun Yu. Simulation analysis of influence of oil bulk modulus on fluctuation of pump source speed[J]. Machinery Design & Manufacture, 2020(3): 47–50 (in Chinese) [李贾宝, 谷立臣, 孙昱. 油液体积弹性模量对柱塞泵转速波动影响机理的仿真分析[J]. 机械设计与制造, 2020(3): 47–50]. doi: 10.19356/j.cnki.1001-3997.2020.03.011.

[16] van Schilfgaarde M, Abrikosov I A, Johansson B. Origin of the Invar effect in iron–nickel alloys[J]. Nature, 1999, 400: 46–49. doi: 10.1038/21848.

[17] Guillaume C E. Invar[J]. Nature, 1933, 131(3314): 658. doi: 10.1038/131658c0.

[18] James J D, Spittle J A, Brown S R, et al. A review of measurement techniques for the thermal expansion coefficient of metals and alloys at elevated temperatures[J]. Measurement Science and Technology, 2001, 12(3): R1–R15. doi: 10.1088/0957-0233/12/3/201.

[19] Wang Xuelian, Tong Peng, Xiong Tingjiao, et al. Low thermal expansion for self-compounded Fe_1Co S over a wide temperature range[J]. Ceramics International, 2023, 49(11): 17977–17983. doi: 10.1016/j.ceramint.2023.02.168.

[20] Kanagaraj S, Pattanayak S. Measurement of the thermal expansion of metal and FRPs[J]. Cryogenics, 2003, 43(7): 399–424. doi: 10.1016/S0011-2275(03)00096-1.

[21] White G K. Thermal expansion at low temperatures[J]. Nature, 1960, 187: 927–929. doi: 10.1038/187927b0.

[22] Masavetas K A. The mere concept of an ideal gas[J]. Mathematical and Computer Modelling, 1989, 12(6): 651–657. doi: 10.1016/0895-7177(89)90350-6.

[23] Strachala D, Hylský J, Frk M. Determination of the temperature coefficient of volume expansion heat - transfer fluids by using refractometer[J]. ECS Transactions, 2015, 70(1): 213–220. doi: 10.1149/07001.0213ecst.

[24] Mikhailov G M, Mikhailov V G, Reva L S, et al. Precision fitting of the temperature dependence of density and prediction of the thermal expansion coefficient of liqiuds[J]. Russian Journal of Applied Chemistry, 2005, 78(7): 1067–1072. doi: 10.1007/s11167-005-0451-4.

[25] Lane C D, Hathcock D J, Leavitt A J, et al. Measurement of the bulk modulus of a liquid using a pump–probe laser technique[J]. The Chemical Educator, 2001, 6(4): 235–237. doi: 10.1007/s00897010489a.

[26] Li Zenghui, Qin Weichao, Wang Juan, et al. Experimental and modeling investigations of density and viscosity for the ternary (*N*-octane + ethylcyclohexane + ethylbenzene) mixtures[J]. Industrial & Engineering Chemistry Research, 2024, 63(10): 4647–4661. doi: 10.1021/acs.iecr.3c04439.

[27] Yin Jianguo, Meng Xianyang, Wu Jiangtao. Vibrating tube densimeter for compressed liquid density measurement[J]. Journal of Engineering Thermophysics, 2012, 33(10): 1659–1662 (in Chinese) [尹建国, 孟现阳, 吴江涛. 高压振动管密度计实验系统研制[J]. 工程热物理学报, 2012, 33(10): 1659–1662].

[28] Paredes X, Fandiño O, Pensado A S, et al. Experimental density and viscosity measurements of di(2ethylhexyl)sebacate at high pressure[J]. The Journal of Chemical Thermodynamics, 2012, 44(1): 38–43. doi: 10.1016/j.jct.2011.07.005.

[29] Nayak A K, Singh R K, Kulkarni P P. Measurement of volumetric thermal expansion coefficient of various nanofluids[J]. Technical Physics Letters, 2010, 36(8): 696–698. doi: 10.1134/S1063785010080055.

[30] Gottsmann J, Dingwell D B, Gennaro C. Thermal expansion of silicate liquids; direct determination using container-based dilatometry[J]. American Mineralogist, 1999, 84(7-8): 1176–1180. doi: 10.2138/am-1999-7-821.

[31] Blagonravov L A, Karchevskii O O, Ivannikov P V, et al. Experience of applying double modulation technique to measure thermal expansion coefficient of conducting fluids[J]. Moscow University Physics Bulletin, 2008, 63(1): 49–54. doi: 10.3103/S0027134908010104.

[32] Kambic M, Kalb R, Tasner T, et al. High bulk modulus of ionic liquid and effects on performance of hydraulic system[J]. The Scientific World Journal, 2014, 2014: 504762. doi: 10.1155/2014/504762.

[33] Tanaka M, Girard G, Davis R, et al. Recommended table for the density of water between 0 C and 40 C based on recent experimental reports[J]. Metrologia, 2001, 38(4): 301–309. doi: 10.1088/0026-1394/38/4/3.

[34] Bigg P H. Density of water in SI units over the range 0-40℃[J]. British Journal of Applied Physics, 1967, 18(11): 1659. doi: 10.1088/0508-3443/18/11/526.

[35] Bahadori A, Vuthaluru H B. Prediction of bulk modulus and volumetric expansion coefficient of water for leak tightness test of pipelines[J]. International Journal of Pressure Vessels and Piping, 2009, 86(8): 550–554. doi: 10.1016/j.ijpvp.2009.01.007.

[36] Botros K K, Crowe J, Liu V, et al. Models for predicting the test medium temperature during hydrotesting pipe segments based on measured ambient and pipe wall temperatures[J]. Journal of Natural Gas Science and Engineering, 2021, 92: 103989. doi: 10.1016/j.jngse.2021.103989.

[37] Ashcroft S J, Booker D R, Robin Turner J C. Density measurement by oscillating tube. Effects of viscosity, temperature, calibration and signal processing[J]. Journal of the Chemical Society, Faraday Transactions, 1990, 86(1): 145. doi: 10.1039/ft9908600145.

[38] Fang Jingbo, Cao Hui, Bai Pengpeng, et al. High-pressure rheological properties of polyalphaolefin and ester oil blends and their impact on lubrication[J]. Tribology International, 2025, 201: 110262. doi: 10.1016/j.triboint.2024.110262.

[39] Fandiño O, Pensado A S, Lugo L, et al. Compressed liquid densities of squalane and pentaerythritol tetra(2-ethylhexanoate)[J]. Journal of Chemical & Engineering Data, 2005, 50(3): 939–946. doi: 10.1021/je049580w.

[40] Fandiño O, Comuñas M J P, Lugo L, et al. Density measurements under pressure for mixtures of pentaerythritol ester lubricants. analysis of a density–viscosity relationship[J]. Journal of Chemical & Engineering Data, 2007, 52(4): 1429–1436. doi: 10.1021/je700121n.

[41] Cui Jinlei, Yang Ping, Liu Xiaoling, et al. A new viscosity-pressure formula for calculating viscosity from density of lubricating oils[J]. Tribology, 2016, 36(1): 13–19 (in Chinese) [崔金磊, 杨萍, 刘晓玲, 等. 由润滑油密度求黏度的新黏压关系式探讨[J]. 摩擦学学报, 2016, 36(1): 13–19]. doi: 10.16078/j.tribology.2016.01.003.

[42] Cui Jinlei, Yang Ping, Liu Xiaoling, et al. A further investigation on the viscosity-density relation of lubricant and a quantitative numerical analysis for the generalized Newtonian thermal EHL problem[J]. Tribology, 2016, 36(6): 679–686 (in Chinese) [崔金磊, 杨萍, 刘晓玲, 等. 润滑油密度与黏度关系的进一步探讨及定量广义牛顿热弹流数值分析[J]. 摩擦学学报, 2016, 36(6): 679–686]. doi: 10.16078/j.tribology.2016.06.003.

[43] Dickmann J S, Devlin M T, Hassler J C, et al. High pressure volumetric properties and viscosity of base oils used in automotive lubricants and their modeling[J]. Industrial & Engineering Chemistry Research, 2018, 57(50): 17266–17275. doi: 10.1021/acs.iecr.8b03484.